

# Kidney Segmentation in Scintigraphic Sequences Data using Multi-Agent Approach

Yassine ARIBI\* and Ali WALI

REGIM-lab: Research Groups in Intelligent Machines, University of Sfax, ENIS, BP 1173, Sfax, 3038, Tunisia.

E-mails: yassine.aribi@ieec.org; ali.wali@ieec.org

\* Author to whom correspondence should be addressed; Tel.: +216 99851139

Received: October 10, 2018/Accepted: May 16, 2019 / Published online: June 30, 2019

## Abstract

**Aim:** The aim of this paper was to define a robust method, allowing the effective detection of structures whose contours change during the time. **Methods:** We integrated an agent model based on a spatiotemporal descriptor for the points of interest detection and Fast Marching Method used for kidney segmentation and tracking in scintigraphic sequences. The proposed agent model contains both type of agents: supervising and explorer agents. As soon as the spatio-temporal descriptors HOG3D detect the points of interest, the supervising Agent create explorer agent on each point of interest in the image. All explorer agents evolve according to the Fast Marching Method. In case of conflict between two agents, the supervising agent should intervene immediately to manage this conflict. **Results:** Our system was applied experimentally on synthetic sequences then on real scintigraphic sequences for the segmentation of the two kidneys. We have found an acceptable performance in the segmentation phase, approved and validated by experts in nuclear medicine. **Conclusions:** Our method achieves high accuracy in kidney segmentation, considerably reducing the time and labor required for contour delineation. In addition, the method can be expanded to 3D segmentation directly without modification.

**Keywords:** Scintigraphic sequences; Segmentation and tracking; Multi-Agent approach

## Introduction

Nuclear medicine is a medical specialty that creates anatomical and functional images of the human body using radioactive substances. The scintigraphic images will be formed once the energy emitted by the radioactive substance administered to the patient is detected. The automatic processing of these images is difficult because of their weak signal and their high noise [1]. For the processing and analysis of scintigraphic images, a software tool would facilitate many tasks. Indeed, in nuclear medicine, segmentation is based on the identification of regions of interest (ROI) which contains all the pixels of a studied structure such as the kidneys for example. The automatic definition of ROI on scintigraphic images constitutes the problem addressed in this paper.

Our work focuses on the ROI detection based on the processing of scintigraphic images. There are two different approaches to analyze such image series, either by following the activity of a region of interest or computing parametric images. Scintigraphic images often suffer from a low contrast and are tainted with noise that makes it difficult to identify their regions of interest [2]. The scintigraphic images present other problems such as interpatient variation and the absence of

anatomical benchmarks. Indeed, to obtain an effective segmentation in nuclear medicine, we must think to pretreat all images in order to overcome all these problems.

Automatically determining the number of regions represents a great challenge in the field of nuclear medicine. In fact, scintigraphic image segmentation represent a low level processing which precedes the stage of analysis and decision.

Its principle consists of subdividing the image into homogeneous and related regions according to a homogeneity criterion which is particularly difficult to define especially in the case of textured regions. Image regions must be delineated in order to identify nuclear medicine image information [3].

Segmentation in nuclear medicine images is more difficult compared to segmentation of Magnetic Resonance (MR) images [4].

In literature several image segmentation approaches have been proposed [5], but some of them can be applied effectively to nuclear medicine images [6]. Image segmentation algorithms are built on one of two basic properties of gray level values: discontinuity and similarity. The basic approach of the first category consists of partitioning an image according to the intensity of sudden changes (such as edges). In the second category the main approaches are based on partitioning an image into similar regions in accordance with a set of predefined criteria [7]. Region growing, clustering and thresholding are examples of methods which belong to this category. Feature sets such as pixel intensities represent the basis of segmentation, which can be used to calculate other features such as texture and edges.

Pixel intensity input comes from a single image since the use of pixel grey scale values in many nuclear images segmentation approaches. The study presented by Rahmatpour et al. in 2014, highlight an automatic approach for kidney ROI identification based on the thresholding method [8]. An automatic thresholding algorithm for kidneys segmentation was developed and presented by Stähl et al. in 2011 [9]. The thresholding techniques limitation is their application to a single band image only, such as single band of a multi-band image or a greyscale image.

The most commonly used algorithms for nuclear medicine are FCM and C-means [10,11]. Hannequin et al. [12] implemented an automated system based on factor analysis and on cluster analysis in a dynamic scintigraphy. Their algorithm suggests first extracting the orthogonal factor images then, these factor images were segmented in ROIs based on hierarchical ascendant classification procedure. Recently, in 2018, Tsujimoto et al. have presented an automated identification of integrated sites in SPECT images resulting from CT images in bone scintigraphy [13].

A semi-automatic segmentation method based on Region Growing algorithm has been used by Aribi et al. in 2012 for the detection of renal ROI in scintigraphic images [14]. In 2013 Aribi et al. have developed another semi-automatic system based on the fast marching method for the segmentation of kidneys ROI in scintigraphic images [15]. Garcia et al. in 2010 have developed an automated image processing algorithm (AUTOROI) to totally generate renal regions of interest (ROI) [16]. Other works proposed also an automatic detection of the ROI in dynamic renal scintigraphy based on the neuron networks RBF [17].

The objectives of the current study are: 1) to develop a robust and intelligent method to automatically detect renal ROI in dynamic study sequences without any expert operator intervention, 2) to use these methods to track renal regions of interest (ROIs), and 3) to evaluate this approach in a large population of subjects with and without suspected renal obstruction.

## **Materials and Methods**

The proposed system consists of the following three fundamental building phases: (1) preprocessing phase (in this first step an adequate filter to reduce the Poisson noise in all images was applied), (2) segmentation phase (a Multi-agent approach based on spatiotemporal descriptor and active contour technique is presented for the segmentation and tracking of scintigraphic images), and (3) tracking phase (the most important step). In fact, the proposed system contains a contour tracking step from one frame to another. The segmentation and tracking phases will be described in the

following sections along with the phases involved and the characteristic features for each processing step. The overall architecture of the introduced system is described in Figure 1.

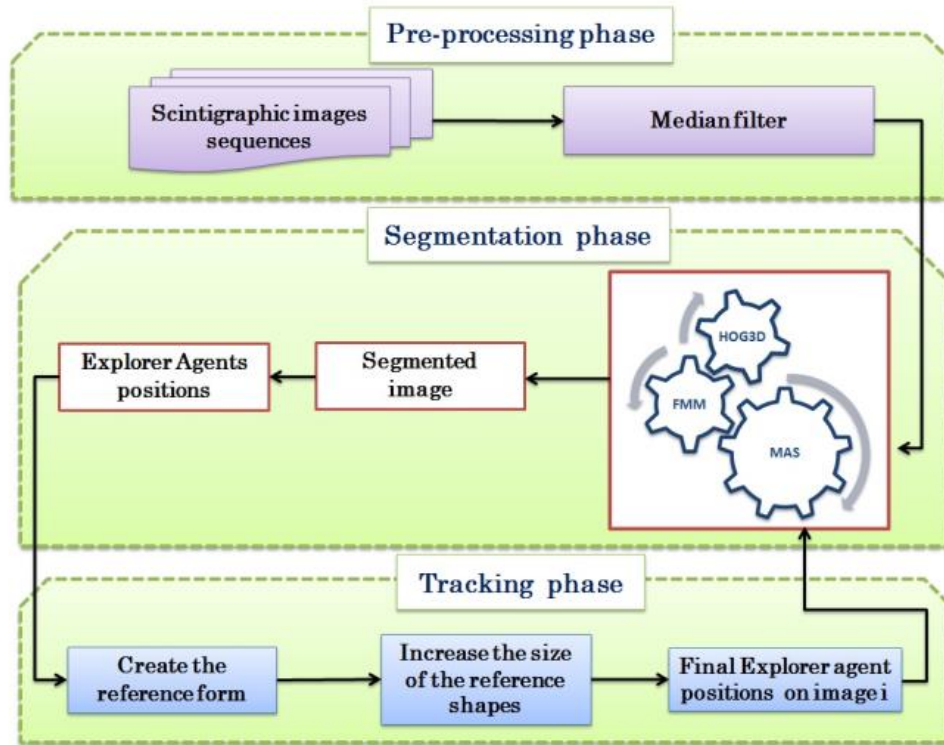


**Figure 1.** An overall architecture of the proposed approach

*Our Multi-Agent Approach*

The purpose of the research on Multi-Agent Systems (MAS) is to find methods and ideas that allow to build complex systems based on autonomous agents which, with limited powers and local knowledge, are capable of providing the desired purpose.

For several years, a particular interest was granted the use of multi-agent systems for the resolution of problems in artificial vision.

Several works propose good solutions to cope with many issues in image segmentation mainly by the parallel processing distribution and solving problems related to data integration and heterogeneous components and distributed [18].

We can note the majority of the proposed MAS for image segmentation are based on a supervised approach [19], and are specific to the content of the processed images.

These systems aim to segment images corresponding to different known objects in previously planned areas. The approach that we propose is rather general and unsupervised.

For our approach, the agent environment consists of two main agent types: Supervising Agent and Explorer Agent. These agents are responsible for the segmentation of the input image. The image processing task includes all the procedures related to the image to alter the input image. The supervising agent creates and initializes the explorer agents, then each explorer agent begins its own task. The supervising agent may decide to create an explorer agent in any different part of image [20].

On the other hand, the supervising agent knows about all the messages which circulate between the explorer agents. It receives their results and it gives orders towards each of them.

All the messages that circulate between the explorer agents are known by the supervising agent. It receives their results and it gives orders to each of them.

For this, the supervising agent must analyses the content of all transmitted messages for power to judge the different situations.

In case of blocking situations or negative results in contour localization, the supervising agent controls the entire process, being capable of making the decision to stop, to continue or to restart the whole process.

The Supervising agent interacts with all the explorer agents. The relationships among the agents are shown in Figure 2.

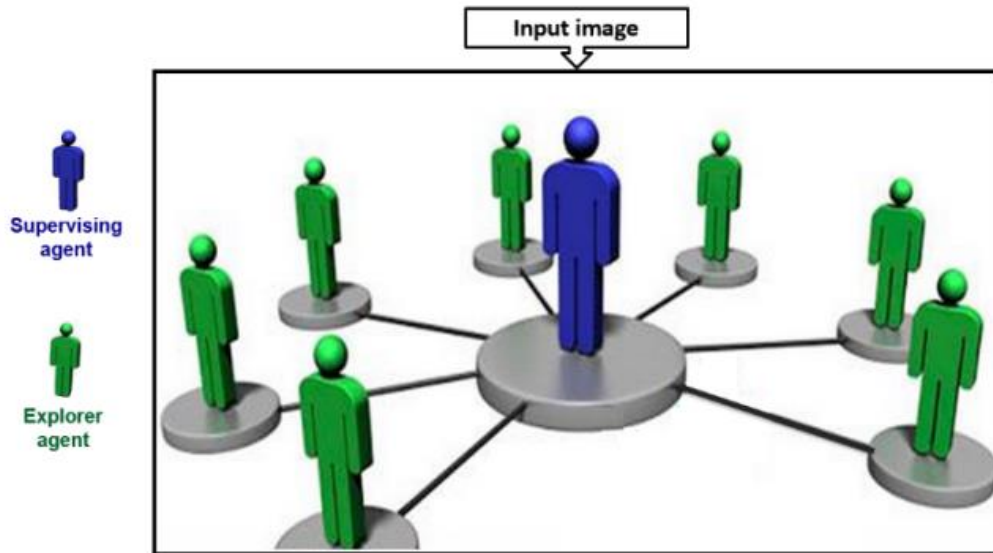


Figure 2. Relationships between roles

*HOG3D Descriptor*

The main goal of the HOG3D descriptor is to find the interest points in the spatio-temporal domain by requiring image values in space-time to have large variations in both the spatial and the temporal directions.

Points with such properties will be spatial interest points with a distinct location in time corresponding to a local spatio-temporal neighborhood with non-constant motion. The spatio-temporal description is usually based on the coupling or 2D + T extension of existing methods such as SIFT or SURF. We studied these descriptors from the referencing published by Wang et al. 2009 [21]. We shall detail the HOG3D introduced by Klaser used in our system [22]. The HOG3D is a spatio-temporal descriptor based on 3D gradient orientations histograms. The different construction phases of the HOG3D descriptor is illustrated in Figure 3.

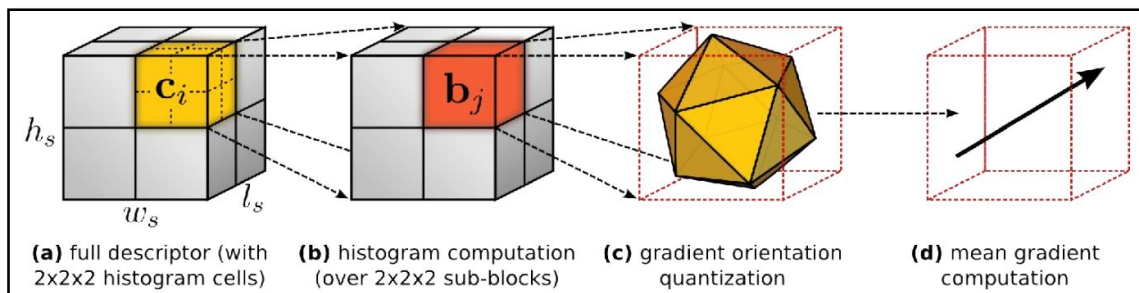


Figure 3. Overview of the HOG3D descriptor

### *Fast Marching Method*

The fast marching method derives from the more general problem of Level Set introduced by [23]. This is a digital interface monitoring technique in an image. The main advantage of this approach is that it assumes no parametric representation of the contour to follow. Thus, it is robust to topology changes (such as a separation into two). However, Level-Set have a very high computational cost.

Indeed, the calculation is performed at all the points of the discretization grid, with each iteration. Fast Marching solves this problem by evaluating the distance in the vicinity of the interface displacement.

The low computational complexity is the main advantage of the Fast Marching Method. This complexity can be simply presented as  $\theta(N\log N)$  where  $N$  represents the total number of points in the region of interest [24].

The FMM algorithm proceeds as follows:

- All points in the initial conditions are tagged as Accepted.
- All pixels in the accepted pixels neighborhood are labeled as Trial.
- The other pixels will be labeled as far.
- The beginning loop: detect the Trial pixel which owns the smallest T value
- Add the chosen Trial pixel to the accepted ones and removed it from the Trial list.
- All the neighbors of the pixel not Accepted chosen in Step 4 will be tagged as Trial.
- All the new Trial pixels values are recalculated.
- Back to Step 4.

### *Our Segmentation and Tracking System Description*

Our system consists of these five steps:

- To divide the video sequence into images.
- To define the points of interest using the descriptor HOG3D,
- The MAS is launched by the supervising and explorer agent activation,
- Each explorer agent is placed on a point of interest detected by HOG3,
- The movement of each explorer agent from one pixel to another is based on the Fast Marching algorithm rules.

Our MAS converges if all the explorer agents can no longer evolve.

Based on the proposed organization we can easily deduce that our system contains two large modules that provide the process of segmenting a scintigraphic images sequence.

The first module is responsible for segmenting the first image of the sequence by applying the techniques of FMM and HOG3D, the second module starts just after detecting the contour of the first image, tracking points of interest on the next frame will be provided by the spatiotemporal descriptor HOG3D. This process requires few iterations to find the contour of the next image using the FMM algorithm.

This process continues to function until the last frame of the sequence in order to obtain the regions of interest on each scintigraphic image.

Figure 4 illustrates in detail our segmentation and tracking process. The use of agents has allowed us to segment the first frame of a video sequence and thus extract the ROI to follow. In fact, the segmentation phase based on our agent method needs a good communication between explorer agents and also sometimes another type of communication with the supervising agent specially in case of occupancy pixel problem.

To achieve this goal, we opt for the exploitation of the powerful characterization of negotiation between supervising and explorer agents. Several negotiation cases are described as follows:

- The two explorer agents ( $i$  and  $i+1$ ) tried to occupy the same pixel.
- The two explorer agents ( $i$  and  $i+1$ ) arrived at the same moment.
- The two explorer agents ( $i$  and  $i+1$ ) have the same distance to the target pixel

The supervising agent has to take a decision in every stage of negotiation.

A detailed description of this negotiation process is explained in the Figure 5.

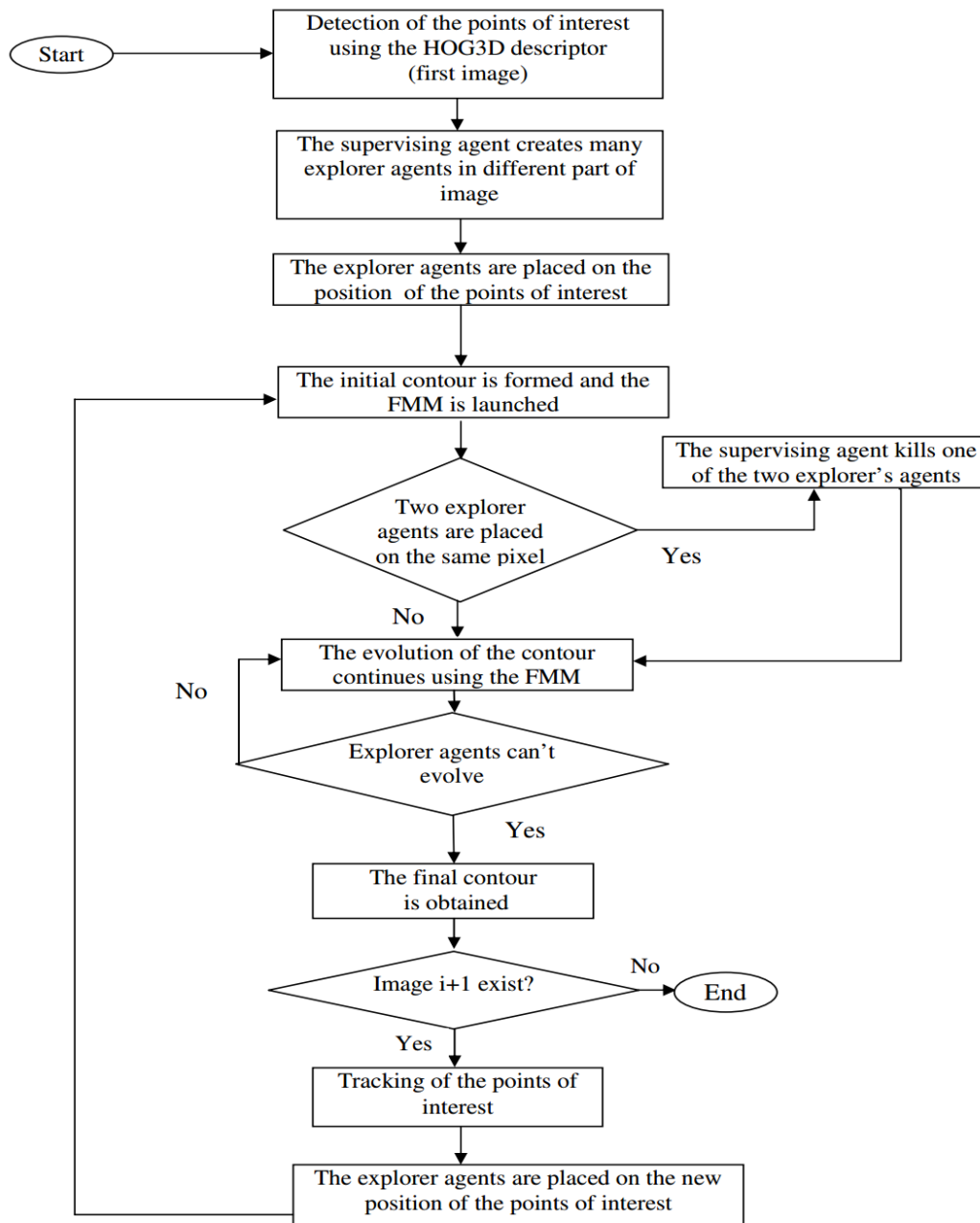


**Figure 4.** Overview of our segmentation and tracking process

The next step is to track ROI in the video. In fact, the segmentation process in our method requires tracking the contours' process (ROI).

The main tasks of agents is the segmentation of the scintigraphic sequence first frame and then the extraction of the ROI. The resulted contour will serve as a reference for the other images. Once the ROI is extracted, the tracking algorithm is as follows:

- Step 1: The agents positions in the previous frame is retrieved and the reference form is created
- Step 2: The size of the reference shapes is increased for a few pixels on all sides.
- Step 3: Perform the segmentation by taking into account initial image  $i + 1$  the final positions of agents in the image  $i$ .

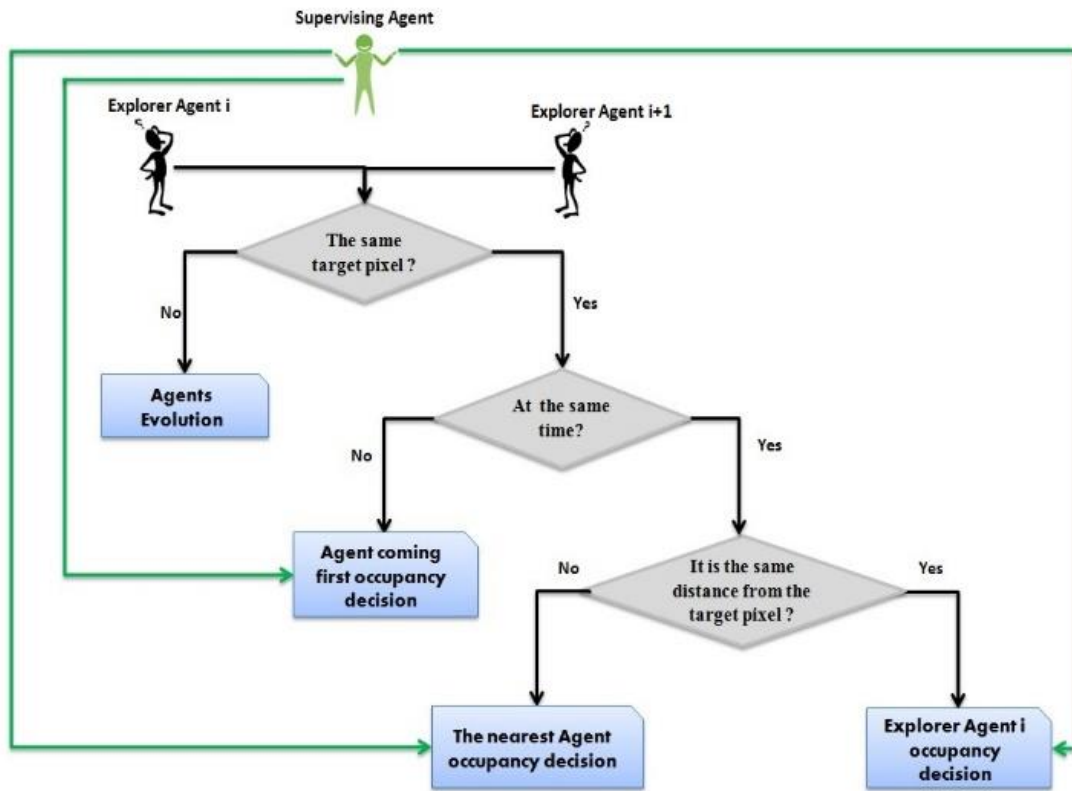


Figure 5. Block diagram of the negotiation between agents

Validation

The proposed method is designed mainly for tracking the spatio-temporal variation of the two kidneys in dynamic renal scintigraphic sequences. The method was first tested on synthetic sequences, in order to verify its effectiveness in an ideal case.

First, we built a database of synthetic sequences, which will serve as training set. We synthesized ten sequences disturbed by Poisson noise. Each sequence contains six images of 128×128 pixels, simulating the variation over time of a simple shape (see Figure 6).



Figure 6. Example of a sequence of the synthetic set simulating the variation over time of a simple shape

We use for the evaluation of our proposed approach two databases of Dynamic Scintigraphic Images. The first database is called “DDRS” (Database of dynamic renal scintigraphy) [25], to obtain a variety of images, the database contains 107 selected adult patients. The second database called “CHRD” (CHU Hospital Renal Database) includes 3600 images from 30 patients, provided by Nuclear Medicine and biophysics Department, CHU Hospital Habib Bourguiba, Sfax, Tunisia. For the two renal databases, most patients had different stages of chronic renal disease. Image data are available in INTERFILE and DICOM formats [26].

To evaluate segmentation results we measure the correspondence between the manual reference given by the experts and the detected contours. We used two different metrics, i.e. the Mean Absolute Distance MAD and the Hausdorff Distance HD.

HD works well to evaluate the local behavior of the algorithm, while MAD measures an overall match between the two contours.

## Results and Discussion

### Results on Synthetic Sequences

Figure 7 shows an example of a result of our segmentation method obtained on a synthetic test sequence. We note that, in all images of the sequence, our system can identify the target shape correctly. The accuracy of this result can be explained by two points. On the one hand, the target contours are quite clear and thus easily detectable. On the other hand, we can say that our algorithm is based on the simplicity of multi-agent system architecture.

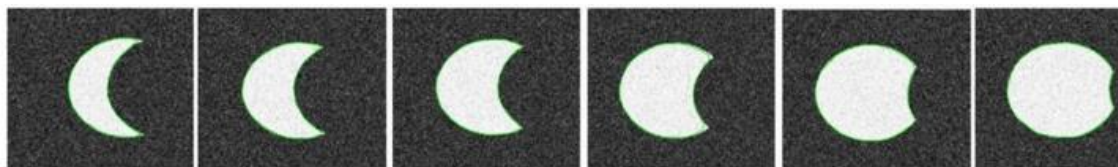


**Figure 7.** Result of the proposed method obtained on a synthetic sequence

Good accuracy of object segmentation is the result of the application of a spatio-temporal descriptor in our multi-agent algorithm architecture. Further, we will apply it in a real case where even the manual tracing of the target contour is difficult.

### Results on Renal Databases

Table 1 provides the standard deviation and mean the error measures achieved for the complete database on the "DDRS". We presented the error measures related to the proposed method (columns 3 and 4) for each measurement (MAD, HD) of the manual method (first two columns).

**Table 1.** Renal scintigraphy segmentation results.

	Manual method		our method	
	MAD	HD	MAD	HD
<b>CHRD</b>	1.08 (0.38)	3.37 (1.16)	1.32 (0.91)	3.74 (2.07)
<b>DDRS</b>	1.56 (0.52)	4.97 (1.44)	1.38 (0.48)	4.14 (1.15)

In "CHRD" (first line of Table 1), we can notice that our method gives small values for both criteria (MAD = 1.32 mm and HD = 3.74 mm). Our segmentation results are therefore very close to the reference contours both on a local (HD) and global (MAD) scale for this orientation.

Moreover, compared to the corresponding manual method (column 1 and 2 of Table 1), it can be concluded that, with the proposed method, the values obtained are closer to those of the expert (respectively 1.08 mm and 3 mm), 37 mm for MAD and HD).

This proves that this segmentation provides coherent results in that the difference with the expert's reference is comparable to the distance between the experts.

This can also be noticed from the standard deviation, since those obtained with our algorithm are very close to those of the experts.

The same conclusions are valid for "DDRS", where the errors obtained (for example, MAD = 1.38 mm) are lower than the manual (MAD = 1.56 mm).

The results of our method and the manual one are shown in term of Hausdorff distance (HD) and Mean Absolute Distance (MAD).

Figure 8 illustrate a qualitative comparison of the obtained results.

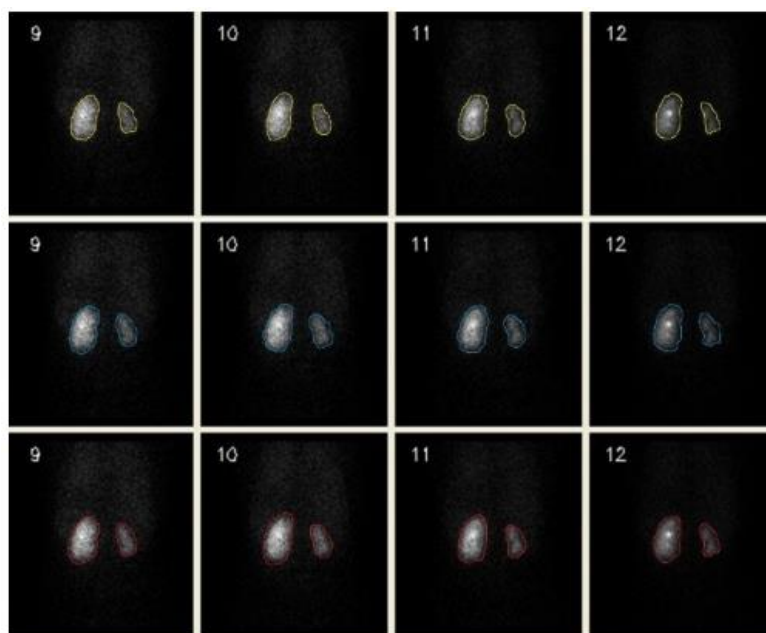


**Figure 8.** Qualitative comparison of results on a renal sequence (Images 9, 10, 11, 12). (First row) Our segmentation method, (Second row) Manual segmentation by expert 1, (Third row) Manual segmentation by expert 2.

In order to perform the evaluation of segmentation algorithms, the automatically segmented images results were compared to those of a manual segmentation called "gold standard".

The expert physicians working at the CHU BOURGUIBA, Sfax, derived the results based on the manual segmentation.

The similarity degree between the machine segmented images and the manually segmented images reflects the accuracy of the segmented image. The performance indices such as accuracy and statistical parameters were used for the segmentation results evaluation.

We chose to compare our method with the ground truth, the Rahmatpour et al. [8] method and with another method proposed by Stähl [9]. As a measure of the segmentation quality we use the Hausdorff distance [27]. This metric is widely used in multiple applications of the medical field. In our case, we used this distance to calculate the similarity between two contours. Figure 8 illustrate the Hausdorff distance between each method (Rahmatpour et al. [8], Stähl et al. [9] and our method) and the reference segmentation of the two sequences.

On each diagram of Figure 9, the horizontal axis represents the images of the sequence and the vertical axis represents the values of the Hausdorff distance. The green curve represents the values of the Hausdorff distance between the automatic segmentation and the manual one obtained by our method. The red curve represents the values of the Hausdorff distance between the automatic segmentation and the manual one obtained by Rahmatpour et al. method [8].

The blue curve represents the values of the Hausdorff distance between the automatic segmentation and the manual segmentation obtained by the Stähl et al. method [9].

Looking at both diagrams, we can clearly notice that the green curve has a slight stability compared to the other curves (blue and red). In fact, through the two diagrams and for the green curve, the Hausdorff values are between 2.13 and 7.68 (mm).

However, the values of the Hausdorff distance for both blue and red curves always represent great variations, which has gone from 4.18 (mm) to 15.78 (mm). Through these comparison measures it can be seen that the Rahmatpour et al. method [8] and the Stähl et al. method [9] give acceptable

results in some cases, but in spite of this we can deduce that our method gives an overall result that is closer to manual segmentation and stable for all the images in both sequences.

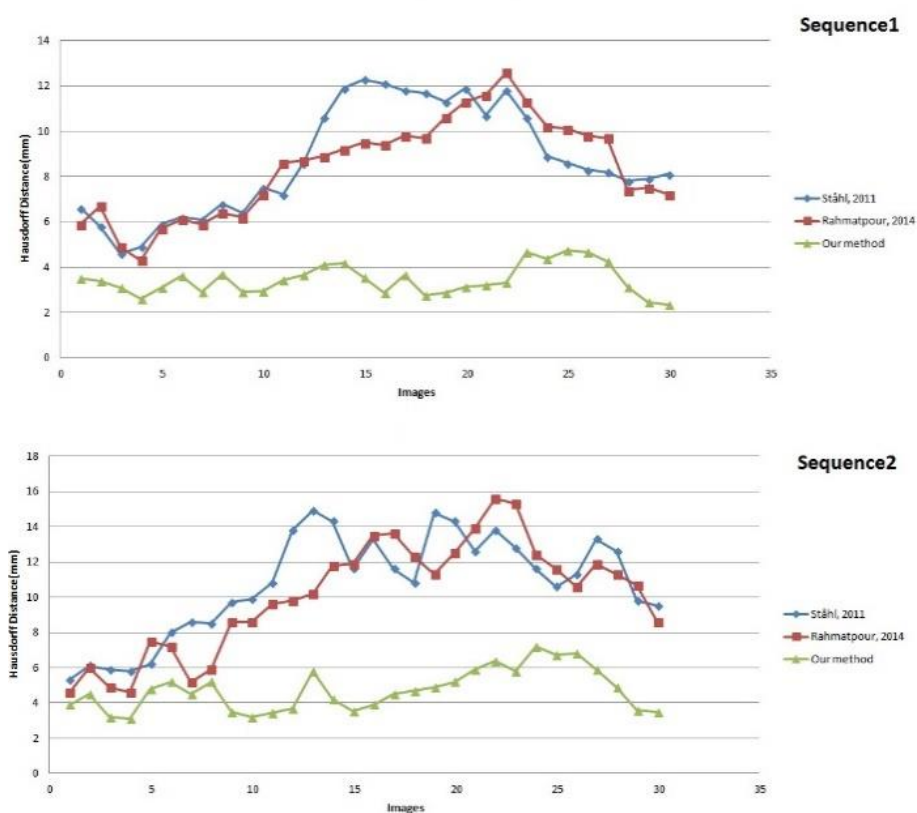


Figure 9. Hausdorff distance results for each method in two sequences.

In conclusion, it is clear that the integration of the uses of MAS in combination with spatiotemporal descriptor with the FMM improved significantly the results of segmentation. This necessarily increases the reliability and effectiveness of diagnostic parameters such as renal function in our case, whose measurement is based on these results. However, we should know that these findings may be enriched to include more sequences in the process of quantitative validation.

The segmentation results of our method can be used to diagnose the kidney diseases and make treatment planning. The results are also useful for 3D visualization.

The obtained methodology may be easily suited and applied to other similar medical applications or adopted in the future to other image processing applications such as video indexing, motion recognition, video surveillance, video communication and compression, human-computer interaction or traffic control.

## Conclusion

In this paper, we proposed a new agent architecture for the segmentation of ROI on dynamic scintigraphic images. The proposed MAS architecture requires the presence of two types of agents, a supervising agent and an explorer agent.

The method was tested on the whole dataset of real cases of patients that were carefully chosen. Experimental results have been shown visually and achieve reasonable consistency. The performance evaluation of segmentation results demonstrates that our kidney segmentation method is accurate and efficient.

## Acknowledgements

The authors would like to acknowledge the financial support of this work by grants from General Direction of Scientific Research (DGRST), Tunisia, under the ARUB program.

## References

1. Bao P, Zhang L. Noise Reduction for Magnetic Resonance Images via Adaptive Multiscale Products Thresholding. *IEEE Trans on Medical Imaging*. 2003;22:1089-1099.
2. Yin T, Chiu N. A computer-aided diagnosis for locating abnormalities in bone scintigraphy by a fuzzy system with a three-step minimization approach. *IEEE Trans on Medical Imaging* 2004;23:639-654.
3. Lyra M, Ploussi A, Georgantzoglou A. MATLAB as a Tool in Nuclear Medicine Image Processing. INTECH Open Access Publisher, 2011.
4. Kläser A, Marsza M, Schmid C. A Spatio Temporal Descriptor Based on 3D-Gradients. *British Machine Vision Conference*, 2008, pp. 995-1004.
5. Acharya J, Gadhya S, Raviya K. Segmentation techniques for image analysis: A review. *International Journal of Computer Science and Management Research* 2013;1(4):166-170.
6. Ma Z, Tavares JM, Jorge RN, Mascarenhas T. A review of algorithms for medical image segmentation and their applications to the female pelvic cavity. *Computer Methods in Biomechanics and Biomedical Engineering* 2010;13(2):235-246.
7. Aribi Y, Hamza F, Wali A, Guermazi F, Alimi A. ARG: A semi-automatic system for ROI detection on Renal Scintigraphic images. *14th International Conference on Hybrid Intelligent Systems*, 2014, pp. 303-308.
8. Rahmatpour M, Rajabi H, Sardari D, Babapour F, Ahmadi S. Semi-Automation of renal region of interest in renography images by thresholding and edge detection. *Romanian Reports in Physics* 2014;66:127-132.
9. Ståhl DD, Aström K, Overgaard NC, Landgren M, Sjöstrand K, Edenbrandt L. Automatic Compartment Modelling and Segmentation for Dynamical Renal Scintigraphies. *Proceedings of the 17th Scandinavian Conference on Image Analysis*, 2011, pp. 557-568.
10. Boudraa A, Mallet J, Besson J, Bouyoucef S, Champier J. Left ventricle automated detection method in gated isotopicventriculography using fuzzy clustering. *IEEE Transactions on Medical Imaging* 1993;12:451-465.
11. Zaidi H, Diaz-Gomez M, Boudraa A, Slosman DO. Fuzzy clustering-based segmented attenuation correction in whole-body PET imaging. *Physics in Medicine and Biology* 2002;47:1143.
12. Hannequin P, Liehn JC, Valeyre J. Cluster analysis for automatic image segmentation in dynamic scintigraphies. *Nucl Med Commun* 1990;11:383-393.
13. Tsujimoto M, Teramoto A, Ota S, Toyama H, Fujita H. Automated segmentation and detection of increased uptake regions in bone scintigraphy using SPECT/CT images. *Annals of Nuclear Medicine* 2018;32(3):182-190.
14. Aribi Y, Wali A, Hamza F, Guermazi F, Alimi A. Analysis of Scintigraphic Renal Dynamic Studies: An Image Processing Tool for the Clinician and Researcher. *International Conference on Advanced Machine Learning Technologies and Applications*. 2012, pp. 267-275.
15. Aribi Y, Wali A, Alimi A. An intelligent system for renal segmentation. *IEEE 15th International Conference on e-Health Networking, Applications Services*. 2013, pp. 11-15.
16. Garcia EV, Folks R, Pak S, Taylor A. Totally Automatic Definition of Renal Regions-of-Interest from Tc-99m MAG3 Renograms: Validation in Patients with Normal Kidneys and in Patients with Suspected Renal Obstruction. *Nucl Med Commun*. 2010;31(5):366-374.
17. Siogkas GK, Dermatas ES. Automating Medical Diagnosis in Renal Scintigrams using RBF Networks. *International Conference from Scientific Computing to Computational Engineering*, 2004, 9 pages.

18. Metzger M, Polakow G. A Survey on Applications of Agent Technology in Industrial Process Control. *IEEE Transactions on Industrial Informatics* 2011;7(4):570-581.
19. Estrada F, Jepson AD. Benchmarking image segmentation algorithms. *International Journal of Computer Vision* 2009;85(2):167-181.
20. Aribi Y, Hamza F, Wali A, Alimi A, Guermazi F. An Automated System for the Segmentation of Dynamic Scintigraphic Images. *Applied Medical Informatics* 2014;34:1-12.
21. Wang H, Muneeb Ullah M, Kläser A, Laptev I, Schmid C. Evaluation of local spatio-temporal features for action recognition. *Proceedings of the British Machine Vision Conference*, 2009.
22. Kläser A, Marszalek M, Schmid C. A Spatio-Temporal Descriptor Based on 3D-Gradients. *British Machine Vision Conference*, 2008, pp. 995-1004.
23. Osher S, A Sethian JA. Fronts propagating with curvature-dependent speed: Algorithms based on Hamilton-Jacobi formulations. *Journal of Computational Physics*, 1998;79(1):12-49.
24. Aribi Y, Wali A, Alimi A. Automated fast marching method for segmentation and tracking of region of interest in scintigraphic images sequences. *International Conference on Computer Analysis of Images and Patterns*. 2015, pp. 725-736.
25. Database of dynamic renal scintigraphy [online]. Available at: URL: <http://www.dynamicrenalstudy.org/>
26. Graham RN1, Perriss RW, Scarsbrook AF. DICOM demystified: A review of digital file formats and their use in radiological practice. *Clinical Radiology* 2005;60:1133-1140.
27. Huttenlocher DP, Klanderman GA, Rucklidge WJ. Comparing images using the Hausdorff distance. *Pattern Analysis and Machine Intelligence* 1993;15:850-863.